# Strongly Subspectral Conjugated Molecular Systems. From Small Molecules to Infinitely Large $\pi$-Electronic Networks

**Jerry Ray Dias**

*Department of Chemistry, University of Missouri, Kansas City, Missouri 64110-2499*

*Received: May 8, 1997; In Final Form: July 14, 1997*[⊗]

Series of molecular graphs having a preponderance of common eigenvalues are identified, and their structural relationships studied. A framework for the analysis of graphitic polymers is provided by an infinite two-dimensional mapping. Collections of subspectral structures (molecular graphs) and their eigenvalues are tabulated for the first time.

The analysis of $\pi$-electronic structure of polymer networks continues to attract the interest of theoretical[1] and synthetic[2−7] researchers. One of the major objectives of these studies is to gain insight on the design of potential organic conductors and ferromagnets. Extended p$\pi$-conjugated systems represent the simplest models for molecular wires. The reduction of the HOMO−LUMO bandgap in conjugated systems will enhance the thermal population of the conduction band and thus increase the number of charge carriers, and minimizing the degree of bond length alternation in a conjugated path which is the origin of Peierls instability will help preserve the proximity or degeneracy between the HOMO−LUMO electronic levels. Thus, researchers need to learn what structural variables control the HOMO−LUMO energy gap and bond length alternation in p$\pi$-electronic systems before organic conductors can be designed. There is no such thing as a ferromagnetic molecule. However, if parallel spin alignment can be induced in molecules, like polymethyleneacetylene, while it is in the condensed phase, a paramagnetic (and possibly a ferromagnetic) material would be produced.[2] Since electron spins tend to align antiparallel to one another, currently no organic ferromagnetic material has yet been designed and synthesized.

Three general theoretical approaches can be identified: study of infinitely long strips, belt-shaped rings, and a series of strips that are progressively incremented (i.e., a homologous series). This latter approach follows more closely the way experimentalists are capable of studying very large molecules and is analogous to the standard methodology in which molecular systems are partitioned into smaller elementary substructures. For example, infinitely long polyacene strips and cyclic polyacene rings have been frequent objects of theoretical study, but are experimentally unknown, whereas members of the homologous acene series from naphthalene to heptacene are known to progressively decrease in stability and ease of experimental manipulation. Nevertheless, these experimental results for smaller homologues along with theoretical molecular modeling studies[1] suggest that polyacenes will be conductive and reactive materials but not ferromagnetic.[8]

By assuming infinitely long polyacenes can be modeled as infinite belt-shaped rings ([∞]cyclacenes), its irreducible substructure can be obtained.[9,10] Hosoya and co-workers have shown that the density of states of cyclic and linear polyene systems having common repetitive units are identical in the infinite limit. Also, they showed that the singular points of the density of states of infinitely large polyenes correspond to the energy levels present in the cyclic dimer (or cyclic monomer in some cases).[10] By a totally different approach, we showed[8] that successive incremental embedding of infinite strips frequently can be used to recognize the existence of a valence band to conduction band energy gap (HOMO−LUMO gap) after just a few iterations. Successive incremental embedding on an infinitely long conjugated polymer strip consists of embedding with successively larger homologous fragments. These approaches suggest that infinite polyacene should have a zero bandgap.

In the model analysis of large finite polyenes by infinite analogue systems, a number of ambiguities arise, particularly in regard to bond alternation. Consider the use of the cyclic boundary condition in the analysis of linear polymeric polyenes. For finite, planar, monocyclic $4n+2$ polyenes, like benzene, there is no tendency toward bond alternation, whereas for finite linear polyenes, like butadiene and hexatriene, significant bond alternation occurs. From resonance theory, monocyclic polyenes with $4n+2$ p$\pi$-electrons have two Kekulé structures ($K = 2$) and linear polyenes have one ($K = 1$). In other words, bond alternation is a linear polyene "end effect" which is assumed to disappear at infinite length. Let us now consider the use of cyclic acene rings in the analysis of linear acenes. Regardless of the number hexagonal rings in the cyclic acene ring $K = 4$, whereas for linear acenes $K =$ #rings + 1. The number of Kekulé structures in the former can be visualized as arising from two cyclic polyenes joined together via every other carbon, and the number of Kekulé structures in the latter can increase without limit. Given this aforementioned, it appears somewhat amazing that both infinite polyene ring systems and linear systems made of the same repeating unit converge to the same density of states. This result suggests that aromaticity disappears in extended $\pi$-electronic systems.[11]

In this paper, the analysis of numerous pairs of series composed of strongly subspectral molecular graphs is presented and some of the aspects discussed above will be further augmented and clarified. An analytical framework for graphitic polymers is established by the pairwise construction of infinite two-dimensional arrays whereby almost-isospectral pairs of molecular graphs are correlated.

## Basic Terminology

A molecular graph is the C−C $\sigma$-bond skeleton representation of a fully conjugated polyene molecule. A molecular graph, therefore, omits the C and H atoms and the C−H and p$\pi$-bonds. Since most polycyclic conjugated polyenes can have more than one arrangement of its p$\pi$-bonds, the molecular graph representation avoids artificially representing these molecular systems by writing only one of these arrangements. Molecular energy level and eigenvalue are equivalent, as are wave function and

[⊗] Abstract published in *Advance ACS Abstracts,* September 1, 1997.

S1089-5639(97)01552-1 CCC: $14.00 

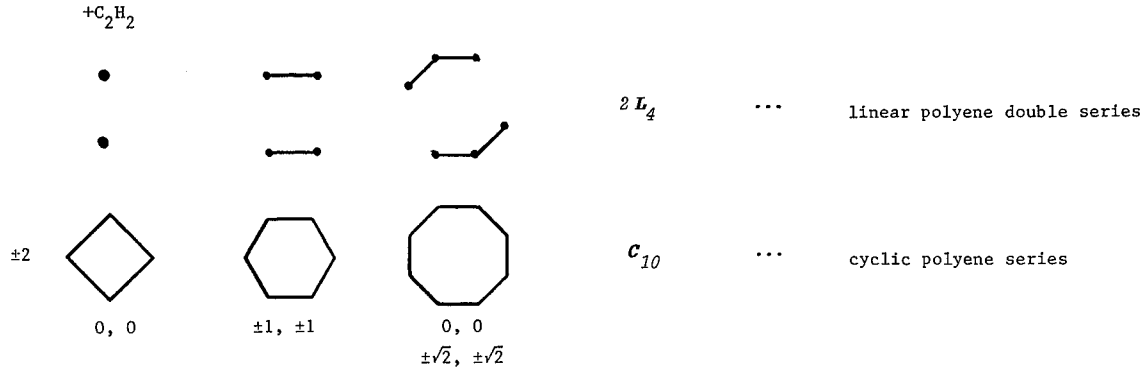


**Figure 1.** Two series of molecular graphs that are almost-isospectral. The unmatched eigenvalues are next to the lower first-generation structure.

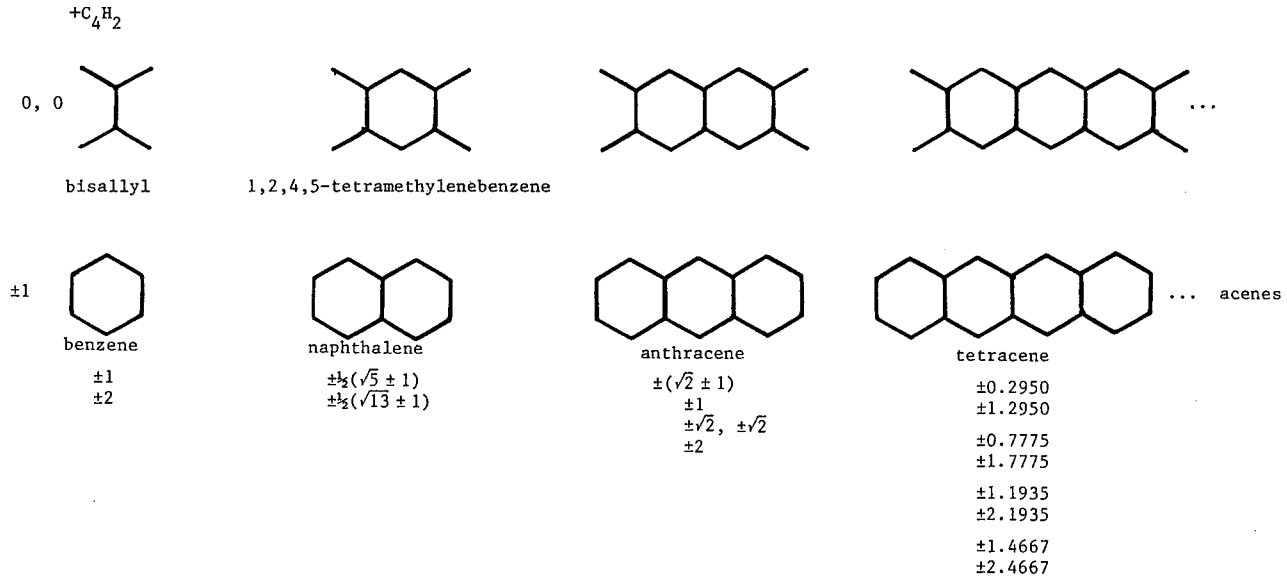


**Figure 2.** Two series of complementary molecular graphs that are also almost-isospectral. The unmatched eigenvalues are indicated at the beginning next to the first-generation structures of each series.

eigenvector. The highest occupied MO (HOMO) and the lowest unoccupied MO (LUMO) are called the frontier MOs (FMOs). An alternant hydrocarbon (AH) is a fully conjugated polyene structure without any odd size rings. In AHs every other carbon vertex can be starred so as no two starred or nonstarred positions are adjacent. Functional groups are substructures (groups of interconnected atoms) having a characteristic set of properties that are conveyed to the whole structure with only minor perturbation. If two molecular graphs have at least one eigenvalue in common, they are said to be subspectral. Two molecular graphs are *strongly* subspectral if they have a preponderance of eigenvalues in common.[12] Two strongly subspectral molecular graphs are *almost-isospectral* if their unique eigenvalues are zero or an integer.[11] The overlapping close proximity of energy levels in infinitely large $\pi$-electronic networks results in bands bounded by singularities.[10] Successive attachment of given aufbau units under prescribed rules can lead to families of molecular graphs having specific characteristics.

## Molecular Orbital Functional Groups

The structural origin of subspectrality among molecular graphs, particularly with commonly recurring eigenvalues, constitutes an area that we refer to as molecular orbital functional groups.[13] Embedding[14] and right-hand mirror-plane fragments[15] are examples of two classes of molecular orbital functional groups. Embedding fragments are called Hall subgraphs,[9,14] and right-hand mirror-plane fragments are called McClelland subgraphs;[9,15,16] McClelland subgraphs have all normal carbon vertexes (type I) or normal carbon vertexes and $-1$ weighted vertexes along the side having bonds severed by the mirror-plane (type II). These MO functional groups are used in similarity comparisons. Strongly subspectral molecules are more similar than molecules without common eigenvalues.

## Almost-Isospectral Series of Conjugated Hydrocarbon Molecules

Through a combination of embedding and mirror-plane fragmentation, one can inductively prove that the series in Figures 1-6 have members that are pairwise almost-isospectral. The unique 0,0, $\pm1$, and $\pm2$ eigenvalue pairs present identically in all members of each relevant series are noted next to the first-generation structures in Figures 1-6. The infinite limit member pairs of these series (Figures 1-6) become, in effect, isospectral, i.e., have the same density of states. Four other pairs of series of molecular graphs that are strongly subspectral, two of which are almost-isospectral, have been reported.[11−12]

## Polyacetylene

Figure 1 summarizes a well-known equivalency between linear and cyclic polyenes which is also expressed by the Frost circle mnemonic. This equivalency is quite evident when the eigenvalues of two identical polyenes are compared with the eigenvalues of a monocyclic polyene having two more carbon vertexes. Both molecular graph sets have the same doubly degenerate eigenvalues with the monocyclic polyene having the additional eigenvalues of $\pm2$. Though the upper infinite series in Figure 1 is comprised of disconnected components, this

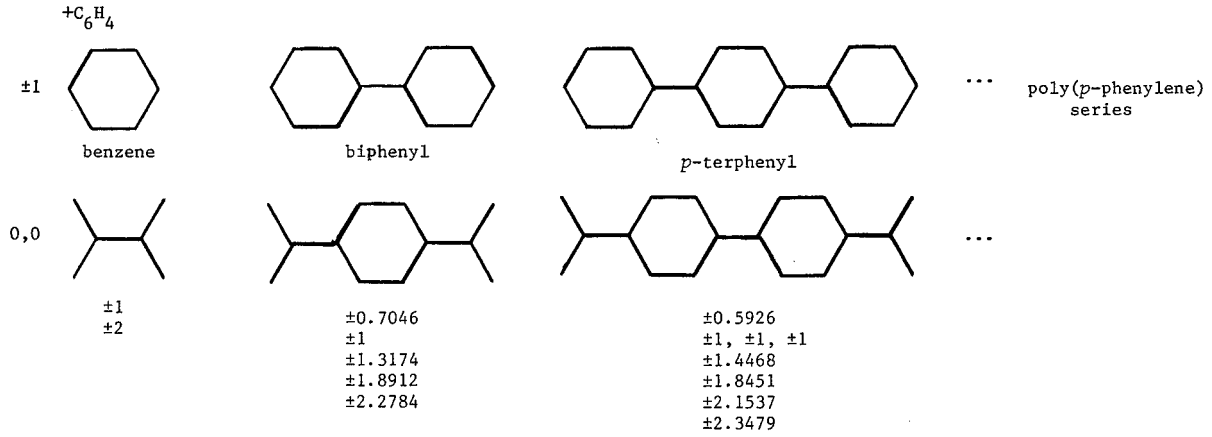


**Figure 3.** Two series of molecular graphs that are almost-isospectral. The unmatched eigenvalues are next to the first-generation structures.

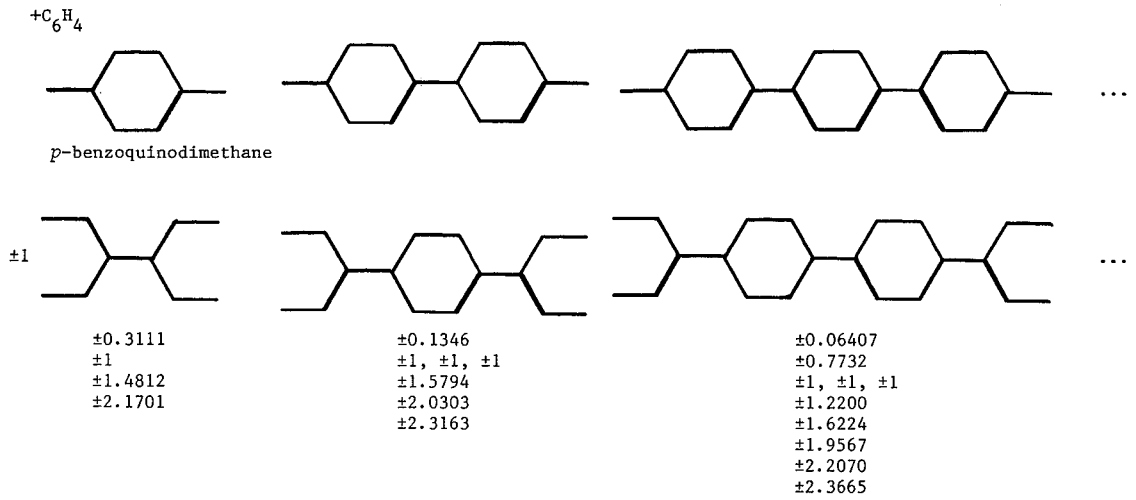


**Figure 4.** Two series of molecular graphs that are almost-isospectral. The unmatched eigenvalues are next to the lower first-generation structure.

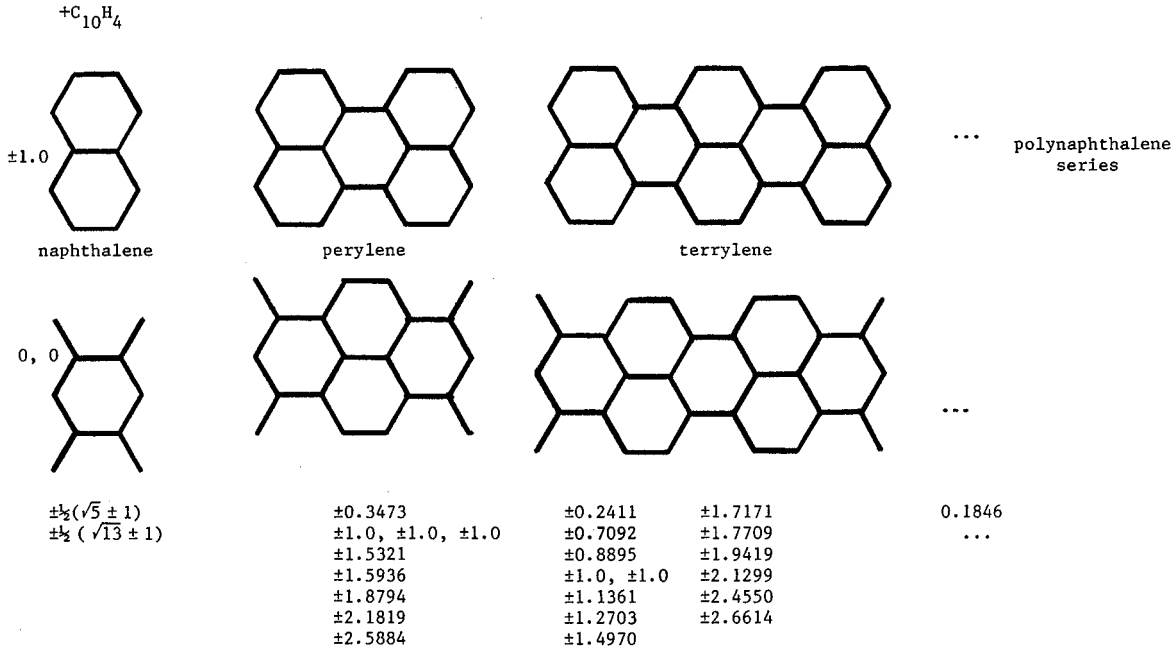


**Figure 5.** Two series of molecular graphs that are almost-isospectral. The unmatched eigenvalues are next to the first-generation structures.

constitutes the simplest example of two series of molecular graphs that are pairwise almost-isospectral. Note that the two linear polyenes in Figure 1 are Hall subgraphs[9,14] of the corresponding monocyclic polyene. This pairwise matching of eigenvalues between the upper and lower molecular graphs of Figure 1 constitutes a proof that both infinitely large linear and cyclic polyenes have the same density of states, in agreement with the work of Hosoya and co-workers.[10]

### Polyacenes

Joining two polyacetylene chains together at every other carbon and dispensing with the detached hydrogens generate

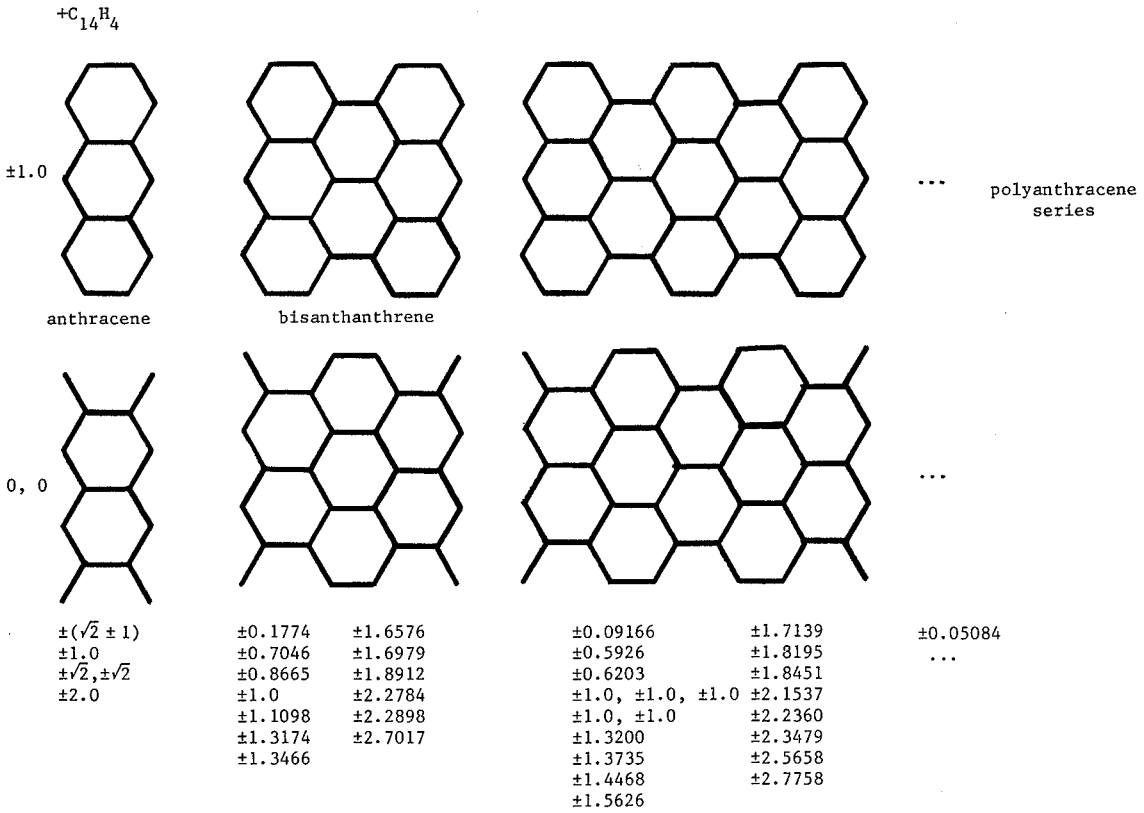


**Figure 6.** Two series of molecular graphs that are almost-isospectral. The unmatched eigenvalues are next to the first-generation structures.

polyacenes, i.e., linear fused benzene rings, the smallest members of which are shown in Figure 2 (bottom series). A large to infinite acene is called polyacene by some investigators.[10] The synthesis of substituted polybenzanthracenes that are intermediate to polyacenes and polyphenanthrenes has been reported by Goldfinger and Swager.[4] Each successive pair of almost-isospectral molecules in Figure 2 differ from the immediately preceding pair by the elementary aufbau unit of $C_4H_2$.[17] Bisallyl is the first generation member of the bisallyl/1,2,4,5-tetramethylenebenzene series in Figure 2, bisallyl/*p*-bisallylbenzene in Figure 3 (lower series), and the bisallyl/[4]radialene series in Figure 4 of ref 11. Subtraction of $C_4H_2$ from the first-generation members in Figure 2 begets two methyl radicals from bisallyl and ethene from benzene, which might be regarded as the zero-generation members of these series. As it will become apparent, the pairs of series in Figures 1-6 are related by a certain consistency and continuity. Each almost-isospectral pair of molecular graphs in Figures 2-6 (and Figure 4 in ref 11) differ by $2\beta$ in $E_\pi$ (i.e., $\Delta E_\pi = 2\beta$). Except for benzene, all the molecular graphs in Figures 1-6 have $D_{2h}$ symmetry. The acene (benzene, naphthalene, etc.) series in Figure 2 have an unmatched $\pm 1$ eigenvalue pair. The initial member molecules in each series are being actively investigated.[18,19] The first- and second-generation diradicals, bisallyl[18] and 1,2,4,5-tetramethylenebenzene,[19] and benzene through heptacene[20] in Figure 2 are known molecular species. Hosoya and co-workers have shown that infinite polyacetylene and polyacenes have zero bandgaps in the absence of Peierls distortion.[10]

All acenes can be embedded by ethene and therefore have the $\pm 1$ eigenvalues of ethene.[9,14,20] The bisallyl/1,2,4,5-tetramethylenebenzene series in Figure 2 have an unmatched zero−zero (0,0) eigenvalue pair because all its members can be embedded two distinct ways by methyl radical.[9,14,20] In Figure 2, bisallyl can be embedded on every other molecular graph of the first series and benzene can be embedded on every other molecular graph of the second series, which results in these systems having the eigenvalues of $\pm 1$ and $\pm 2$. Similarly, 1,2,4,5-tetramethylenebenzene (2,3,5,6-tetramethyene-1,4-cyclohexyldiyl) can be embedded on every third molecular graph in the first series and naphthalene can be embedded on every third molecular graph in the second series. The third-generation molecular graphs in Figure 2 can be embedded on every fourth molecular graph of the corresponding series, the fourth-generation molecular graphs on the fifth molecular graph, and so on. Through a combination of mirror-plane fragmentation[15] and embedding, it is easy to inductively prove that all the members of the two series are pairwise almost-isospectral and that their right-hand mirror-plane fragments are almost-self-complementary.[16] All the diradicals in Figure 2 are reactive species and have disjoint NBMOs.[18] Benzene is the prototype molecule for aromaticity, and it has been shown that resonance energy (RE) contributions decrease rapidly with increasing circuit size and the additional RE per acene ring decreases.[21,22] The calculation and theory of REs for nonradical benzenoids and monoradical AHs is well developed, but the calculation of REs for diradical and higher polyradical systems has not been accomplished. As the number of acene rings increases, the corresponding HOMO values decrease, approaching zero, resulting in progressively more reactive acenes. For example, heptacene is so reactive that it has not been completely characterized and octacene is currently unknown.[20] Thus, the chemistry of the members of the two series in Figure 2 are approaching each other and the infinite limit members of the two series are isospectral, i.e., have the same density of states.

## Polyphenylenes

Figures 3 and 4 present two pairs of almost-isospectral series that in the infinite limit reduce to the same linear polyphenylene polymer but with dramatically different end effects. The first two generation structures in Figure 3 are benzene and bisallyl, exactly the same first generation structures as found in Figure 2 but oriented differently by 90°. The aufbau unit for generation of successive structures in Figures 3 and 4 is $C_6H_4$ compared

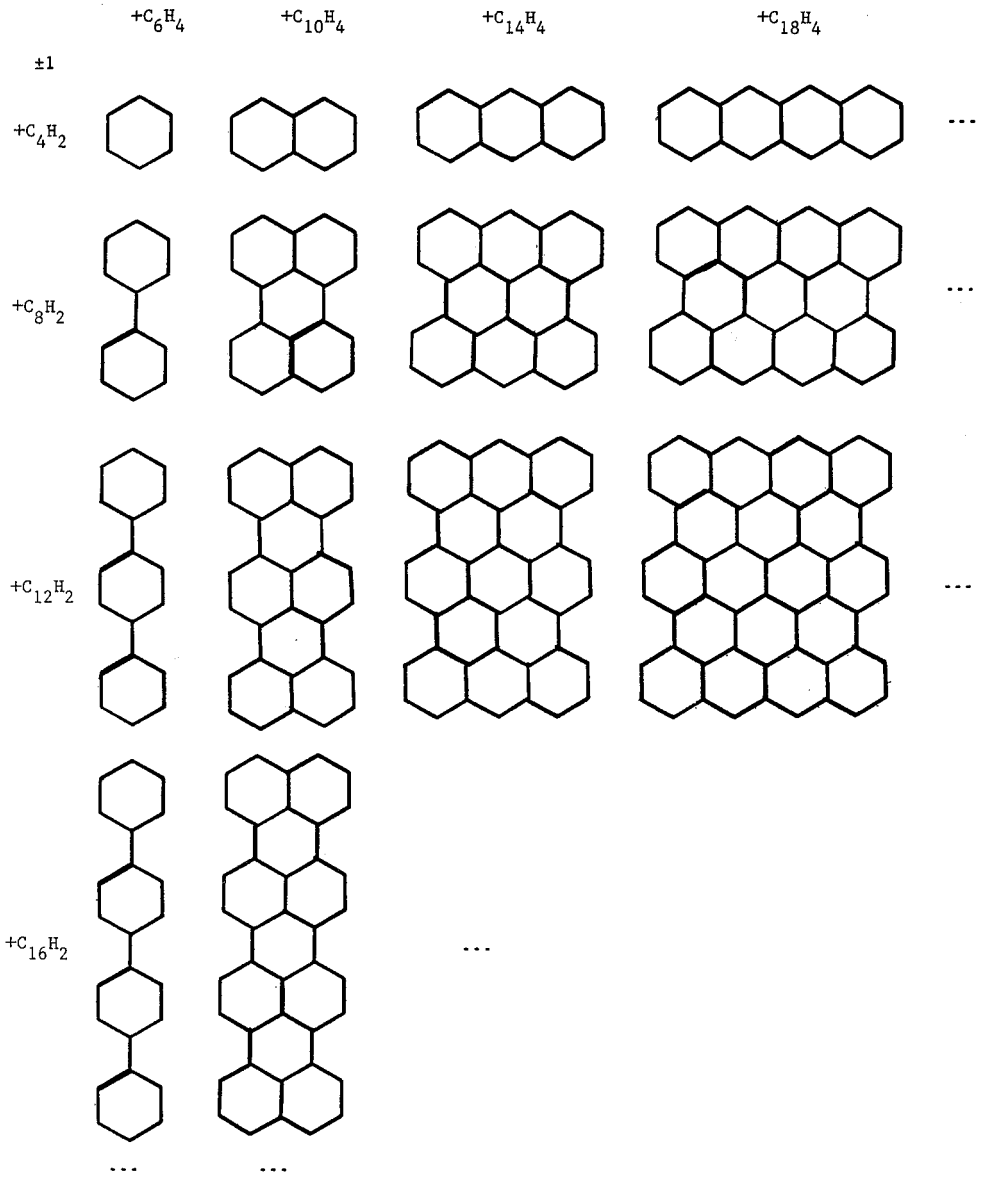


**Figure 7.** Two-dimensional array of molecular graphs that are almost-isospectral to the corresponding molecular graphs given in Figure 8.

to $C_4H_2$ for the structures of Figure 2. As shown by Hosoya and co-workers and Hall and Arimoto,[10] infinite poly(*p*-phenylene), the limit member of the upper series in Figure 3, has a nonzero bandgap and is expected to be nonconductive. Since infinite poly(*p*,*p*-bisallylphenylene), the limit member of the lower series in Figure 3, has the same density of states, it is also expected to be nonconductive; note that its doubly degenerate zero level contains only two electrons, which makes an insignificant contribution compared to the remaining infinite number of electrons. In this case, the bisallyl end effect is negligible and can be disregarded. The results of Figure 4 demonstrate that some types of end effects can be significant. The quino structures in Figure 4 cannot have equivalent cyclic structures for obtaining the singular points of the density of states per the method of Hosoya and co-workers.[10] Quino structures are characterized by a greater degree of bond alternation. While the limit members of the series in Figure 4 are also polyphenylenes, the quino type of end effect makes a substantial contribution, causing a dramatic change in the density of states, for the series in Figure 4 have a zero bandgap and are expected to be electrically conductive. Hall and Arimoto have studied the poly(*p*-phenylene) series (Figure 3) and the poly(*p*,*p*-phenoquinodimethane) series (Figure 4).[10]

Synthetically known poly(*p*-phenylene) has a degree of polymerization of approximately 15 phenyl moieties.[7] It has been shown that this polymer has its rings nearly coplanar, leading to good crystallinity and intercalation properties.[5] Doped poly(*p*-phenylene) has been studied for use as electrochemically active electrodes in rechargeable batteries.[6] Infinite poly(*p*-phenylene) in Figure 3, unlike infinite polyacetylene (Figure 1) and polyacene (Figure 2), has been shown to have a significant nonzero bandgap, but yet finite polymers of poly(*p*-phenylene) are being made conductive by doping.[6] This can be explained as an end effect that cannot occur in polyacetylenes or polyacenes by the results in Figure 4. Oxidants could convert poly(*p*-phenylene) to the following poly(*p*,*p*-phenoquinodimethane) system, which is isoelectronic to the first series in Figure 4.

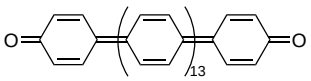


Alternatively, if XY adds to a large poly(*p*-phenylene), one would get the following system which is isoelectronic to the second series in Figure 4.

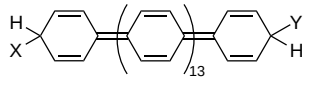

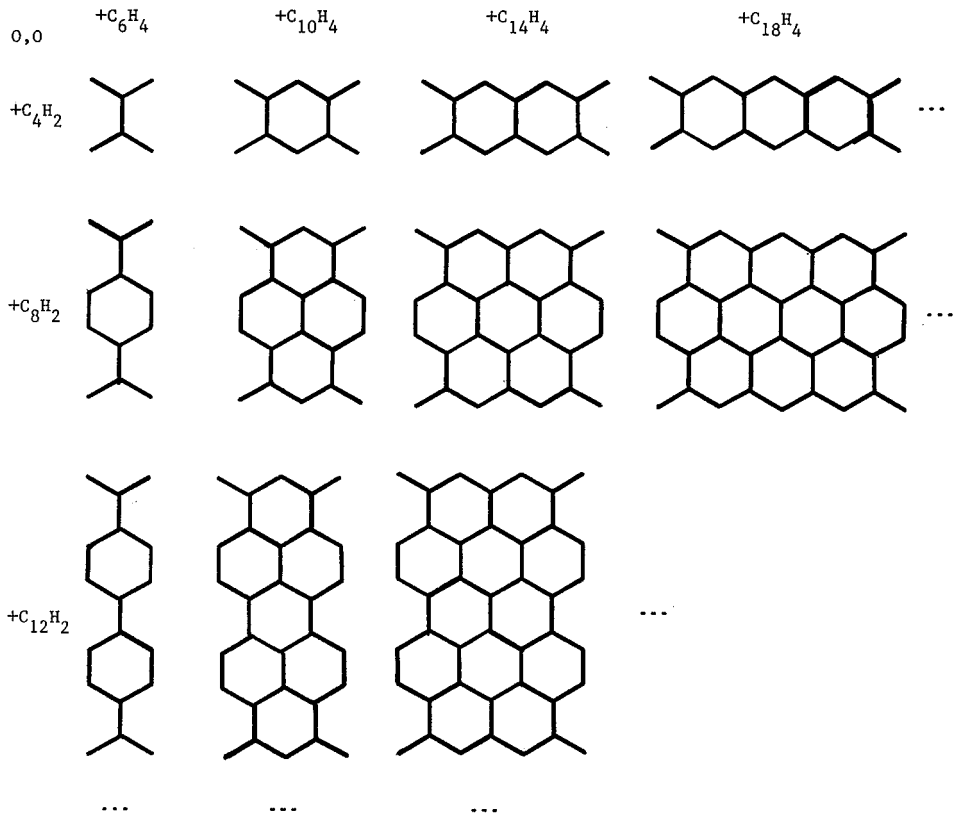


**Figure 8.** Two-dimensional array of molecular graphs that are almost-isospectral to the corresponding molecular graphs given in Figure 7.

Both series in Figure 4 are predicted to become conductive in the infinite limit just as polyacetylene and polyacene are predicted to become conductive. Thus, doping poly(*p*-phenylene) not only changes its electron population but also converts it to a quino type system.

### Polynaphthalene

Polynaphthalene (also referred to as polyperylene and poly(perinaphthalene)) has been theoretically studied by Hosoya and co-workers and Hall and Arimoto.[10] The upper molecular graph series in Figure 5 display the smallest polynaphthalene members; the infinite limit member of this series is predicted to have a zero bandgap.[10] Naphthalene, perylene, terrylene, and quaterrylene are known benzenoids.[20] Polynaphthalene is thought to result when 3,4,9,10-perylenetetracarboxylic anhydride is pyrolyzed[5] and during electrochemical polymerization of naphthalene.[6] Figure 5 also presents another molecular graph series that is almost-isospectral to the polynaphthalene series. Mirror-plane fragmentation (through the long axis except for the first generation structures) of any member of either series in Figure 5 generates a type I McClelland subgraph (without $-1$ weighted vertexes) which is identical with the corresponding member of the polyacetylene series; alternatively, any member of either series in Figure 5 is embeddable by the corresponding member of the polyacetylene series. Since the infinite limit member of the polyacetylene series has a zero bandgap, then the limit member of both series in Figure 5 must also have a zero bandgap. In the same way mirror-plane fragmentation of the infinite limit member of the polypentacene series gives polynaphthalene as a type I McClelland subgraph and, equivalently, has a polynaphthalene Hall subgraph; therefore, infinite polypentacene has a zero bandgap. The same is true for polyoctacene, polyundecacene, and so on (per modulo-3). This is in agreement with the work of Hosoya and co-workers.[10] Klein and co-workers[24] and Gao and Herndon[25] have shown that nonhelical (principal axis of the tube is parallel to two sides of each hexagon) buckytubes with a circumference of $3R$ hexagonal rings ($R$ is an integer) have zero HOMO$-$LUMO bandgaps; all other nonhelical buckytubes always have nonzero bandgaps. These results can be ascertained by mirror-plane fragmentation and/or embedding methods discussed above. For example, partial mirror-plane fragmentation of an $R = 1$ nonhelical buckytube or mirror-plane fragmentation of an $R = 2$ buckytube both give polynaphthalene. For helical buckytubes with a pitch of 1, the circumference selection rule for a zero bandgap is $3R + 1$.

### Polyanthracene

Polyanthracene has been studied by Hosoya and co-workers[10] and is thought to be synthesized during electrochemical polymerization of anthracene.[6] The infinite limit members of the polyanthracene and polytetracene (polynaphthacene) series are predicted to have nonzero bandgaps.[10] Figure 6 presents the smallest members of the polyanthracene series and another series whose members are pairwise almost-isospectral. Mirror-plane fragmentation of any member of the polyanthracene series through their long axis gives a member of the polyphenyl series which also has a nonzero bandgap. Equivalently, any member of the polyanthracene series can be embedded by the same generation member of the polyphenyl series. Thus, polyphenyl is both a McClelland and Hall subgraph of polyanthracene.

Proof that end effects of infinitely long conjugated polymers can under certain circumstances be legitimately disregarded is given by the fact that the six pairs of series previously discussed[10] and those in Figures 1-6 become isospectral (same density of states) and *identical* in the infinite limit by virtue of this assumption.

### Infinite Two-Dimensional Motifs of Almost-Isospectral Series

Using the aufbau principle,[17] the results given in Figures 1-6 can be generalized through the construction of Figures 7 and 8.

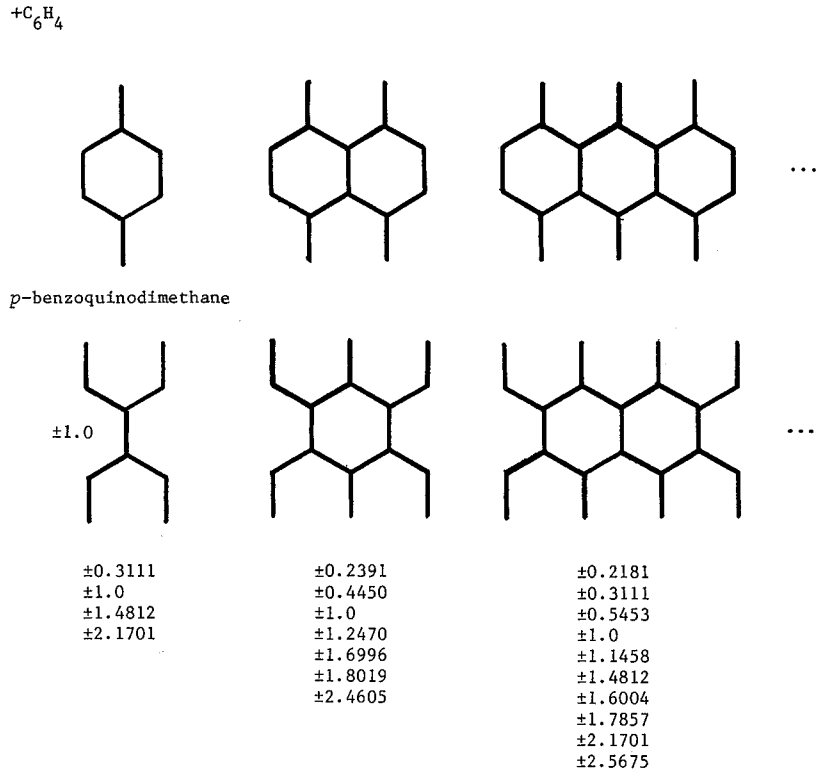


**Figure 9.** Two series of molecular graphs that are almost-isospectral. The unmatched ±1 eigenvalues are indicated next to the first-generation member of the lower series.

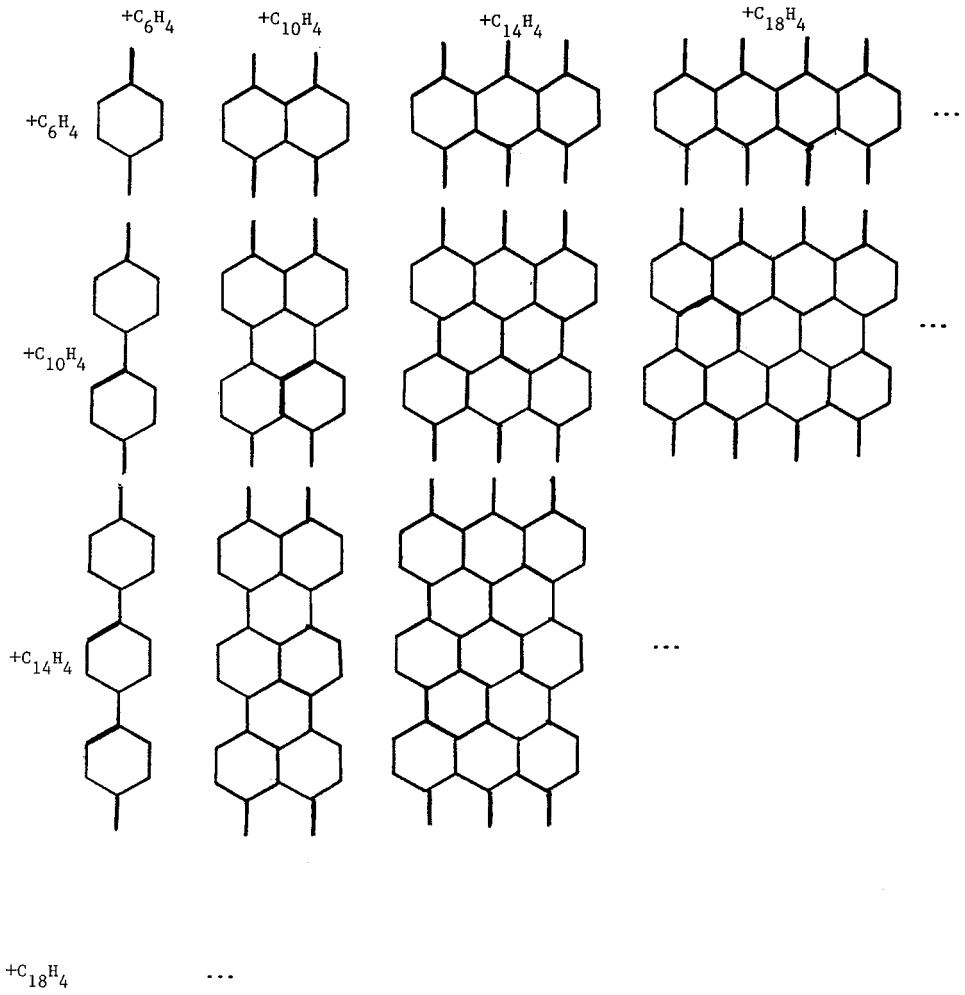


**Figure 10.** Two-dimensional array of molecular graphs that are almost-isospectral to the corresponding molecular graphs given in Figure 11.

Every member of a given column in Figure 7 is almost-isospectral to the corresponding generation member of the same column in Figure 8. Similarly, every member of a given row in Figure 7 is almost-isospectral to the corresponding generation

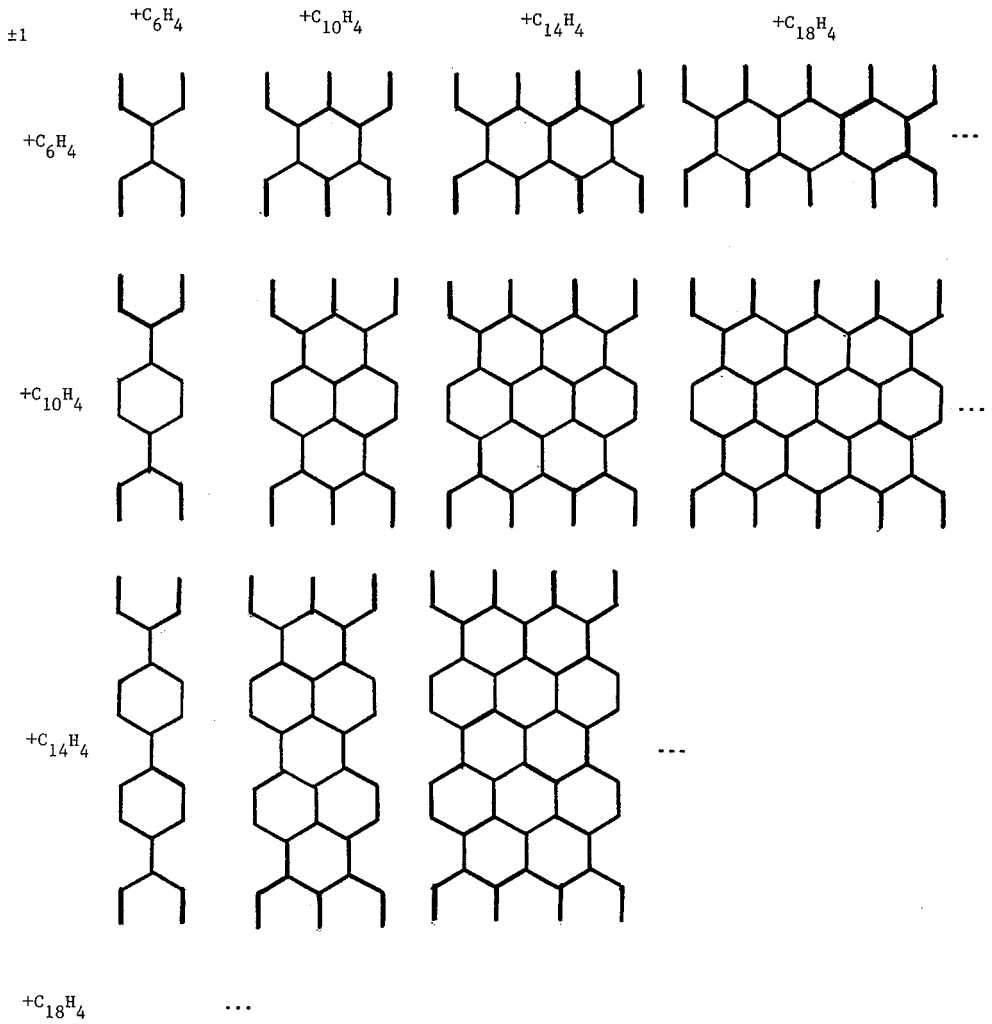


**Figure 11.** Two-dimensional array of molecular graphs that are almost-isospectral to the corresponding molecular graphs given in Figure 10.

member of the same row in Figure 8. Since the columns and rows of Figures 7 and 8 extend indefinitely, these figures contain an infinite number of series having molecular graphs that are pairwise almost-isospectral; for any given isospectral pair, the molecular graph in Figure 7 has a distinct eigenvalue pair $\pm 1$, and its molecular graph counterpart in Figure 8 has a distinct doubly degenerate eigenvalue set of 0,0. The plus formula heading each column and row in Figures 7 and 8 identify the formula of the aufbau unit used to generate all successive molecular graphs in a column or row.

The bandgaps of the limit members to every row series in Figure 7 were deduced to be zero by Hosoya and co-workers,[10,33] whereas the bandgap is zero only for the limit members of the second, fifth, eighth, and so on (per modulo-3) columns. Since the limit member of every row makes up the limit column which by necessity must be made up of all members with zero bandgaps, it is deduced that the nonzero bandgaps associated with the limit members of each non modulo-3 column also approach a zero bandgap as one moves to the right in Figure 7. All the remarks of this paragraph equally apply to almost-isospectral counterparts listed in Figure 8.

Only the three largest molecular graphs (in the second and third rows) explicitly shown in Figure 7 correspond to currently unknown molecules.[20] In comparison, only the two smallest molecular graphs in Figure 8 correspond to molecules that have been experimentally studied (i.e., bisallyl and 2,3,5,6-tetramethylen-1,4-cyclohexyldiyl) at low temperature by photolytic generation in glassy matrixes.[19,26] This is because all the molecular graphs in Figure 8 correspond to disjoint diradical molecules of high reactivity.[18,27] Another property of note is that each molecular graph in Figure 8 is an excised internal structure[17] of some molecular graph in Figure 7. Previously we showed that circumscribing nondisjoint diradicals, like trimethylenemethane diradical, lead to nondisjoint diradical benzenoids, whereas circumscribing disjoint diradicals, like bisallyl, generates closed-shell benzenoids.[28,29] Here again it should be observed that circumscribing any of the disjoint diradicals in Figure 8 gives the corresponding closed-shell benzenoid in Figure 7. The molecular graphs in the first row and column of Figure 7 have no (connected) excised internal structures. In general, within a given set of benzenoid isomers, those having disjoint excised internal structures will have among the smallest HOMO values.

Our previous results list a "formula periodic table for total resonant sextet benzenoid hydrocarbons,"[31] and list all the structures of all essentially strain-free total resonant sextet benzenoids having up to 60 carbon atoms.[20] Total resonant sextet benzenoids have a maximum number of rings ($r_{\text{sextet}} = N_c/6$) covered by resonant sextets (rings having three mutually permutable p$\pi$-bonds). Within their respective isomer sets, total resonant sextet benzenoids have the largest HOMO and $E_\pi$ values. Figure 7 now lists all benzenoids which contain the fewest resonant sextets, many which were identified by Hosoya and co-workers.[30] All the polyacenes in the first row of Figure 7 have only one resonant sextet and represent the least stable isomer with the smallest HOMO values for a given catacondensed benzenoid formula. All the benzenoids in the second row have a maximum of two resonant sextets, in the third row have three resonant sextets, and so on.[30] These benzenoids have

the fewest resonant sextets and among the smallest HOMO values for their respective isomer sets. Benzene and biphenyl in Figure 7 have a provisional status in our formula periodic table for total resonant sextet benzenoids.[31] The benzenoid structures below the first row in Figures 7 and 8 have essential single bonds separating the acene substructures, and all the structures in Figure 8 additionally have essential single bonds between the linear radical chain substructure and benzenoid substructure (or another linear radical chain substructure in the case of the first row series).

Starting with the first generation structures of *p*-benzoquinodimethane and 3,4-diethenyl-1,3,5-hexatriene given in Figure 4 but oriented differently by 90°, the almost-isospectral series given in Figure 9 is obtained. The graphitic polymer strips corresponding to the first (upper) series in Figure 9 were analytically investigated by Klein[32] and Hosoya and co-workers;[33] the limit members of both these series are predicted to have a nonzero bandgap. Figures 10 and 11 generalize the results of Figures 4 and 9 and tallies an infinite number of related almost-isospectral series of molecular graphs. The molecular graphs in Figures 4, 9, 10, and 11 all have $K = 1$. We predict that the limit member to all the column series in Figures 10 and 11 will have a zero bandgap.

## Conclusion

By a completely different approach, this work has identified the differences and similarities that exist between molecular graphs belonging to graphitic networks and their precursors. Specifically, an infinite two-dimensional array containing a family of benzenoid structures can be mapped against another two-dimensional array containing a related family of structures establishing a pairwise almost-isospectral relationship between their corresponding membership. HMO bandgaps and eigenvalues, excised internal structures, and the maximum number of resonant sextets are correlated by this mapping.

Hosoya and co-workers have derived analytical expressions for cyclic analogues of the acene series in Figure 2, polynaphthalene series in Figure 5, and polyanthracene series in Figure 6, which are only valid in the infinite limit for the linear series having the same repeating unit (aufbau unit).[10] Thus, infinite cyclic and linear $\pi$-electronic polymers with common repetitive units have the same density of states. Using Hosoya's method,[10] it can be shown that each pair of series in Figures 2, 5, and 6 give the same cyclic monomeric analogue and therefore previously derived analytical expressions.[10] While analytical expressions can generally be formulated for cyclic polymers, finite linear polymers are generally more easily treated by numerical and algorithmic methods. This work employs the latter approach, which because of its greater simplicity has revealed new insights.

While the sole example of an isospectral (odd carbon) benzenoid pair has only recently been discovered,[34] this work demonstrates that almost-isospectral pairs which include benzenoids as members are far more numerous. Although, the smaller precursors to graphitic networks can look quite different, as their size increases they begin to look more similar and in the infinite limit become virtually identical. This work is a contribution toward the development of a unified structure theory of conjugated polycyclic hydrocarbons.[35,36]

## References and Notes


(1) Gutman, I.; Hosoya, H.; Babic', D. *J. Chem. Soc., Faraday Trans.* **1996**, *92*, 625−628. Li, S.; Ma, J., Jiang, Y. *J. Phys. Chem.* **1996**, *100*, 4775−4780. Hosoya, H.; Harary, F. *J. Math. Chem.* **1993**, *12*, 211−218. Klein, D. J.; Herndon, W. C.; Randic', M. *New J. Chem.* **1988**, *12*, 71−76. Seitz, W. A.; Klein, D. J.; Graovac, A. *Stud. Phys. Theor. Chem.* **1988**, *54*, 157−171.

(2) Baumgarten, M. *Acta Chem. Scand.* **1997**, *51*, 193−198. Graham, R. J.; Paquette, L. A. *J. Org. Chem.* **1995**, *60*, 5770−5777. Matsuda, K.; Nakamura, N.; Takahashi, K.; Inoue, K.; Koga, N.; Iwamura, H. *J. Am. Chem. Soc.* **1995**, *117*, 5550−5560. Rajca, A. *Chem. Rev.* 1994, *94*, 871−893. Allinson, G.; Bushby, R. J.; Paillaud, J.-L. *J. Mater. Sci.: Mater. Elec.* **1994**, *5*, 67−74. Dougherty, D. A. *Acc. Chem. Res.* **1991**, *24*, 88−94.

(3) Tolbert, L. M. *Acc. Chem. Res.* **1992**, *25*, 561−568.

(4) Goldfinger, M. B.; Swager, T. M. *J. Am. Chem. Soc.* **1995**, *116*, 7895−7896.

(5) Roncali, J. *Chem. Rev.* **1997**, *97*, 173−205.

(6) Novak, P.; Muller, K.; Santhanam, K. S. V.; Haas, O. *Chem. Rev.* **1997**, *97*, 207−281.

(7) Kovacic, P.; Jones, M. B. *Chem. Rev.* **1987**, *87*, 357−379.

(8) Dias, J. R. *MATCH* **1987**, *22*, 257−268.

(9) Dias, J. R. *Molecular Orbital Calculations Using Chemical Graph Theory*; Springer-Verlag: New York, 1993.

(10) Hosoya, H.; Aida, M.; Kumagai, R.; Watanabe, K. *J. Comput. Chem.* **1987**, *8*, 358−366. Hosoya, H.; Tsuchiya, A. *J. Mol. Struct.* (*THEOCHEM*) **1989**, *185*, 123−137. Gao, Y.-D.; Hosoya, H. *Theor. Chim. Acta* **1991**, *81*, 105−123; *J. Mol. Struct.* (*THEOCHEM*) **1990**, *206*, 153−172. Hosoya, H.; Kumazaki, H.; Chida, K.; Ohuchi, M.; Gao, Y.-D. *Pure Appl. Chem.* **1990**, *62*, 445−450. Hall, G. G.; Arimoto, S. *Int. J. Quantum Chem.* **1993**, *45*, 303−328.

(11) Dias, J. R. *Chem. Phys. Lett.* **1996**, *253*, 305−312.

(12) Dias, J. R. *J. Mol. Struct.* (*THEOCHEM*), in press.

(13) Dias, J. R. *Mol. Phys.* **1995**, *85*, 1043−1060. *J. Chem. Inf. Comput. Sci.* **1996**, *36*, 356−360.

(14) Hall, G. G. *Bull. Inst. Math. Appl.* **1981**, *17*, 70−72. *J. Math. Chem.* **1993**, *13*, 191−203.

(15) McClelland, B. J. *J. Chem. Soc., Faraday Trans. 2* **1974**, *70*, 1453−1456. *J. Chem. Soc., Faraday Trans. 2* **1982**, *78*, 911−916.

(16) Dias, J. R. *Mol. Phys.* **1996**, *88*, 407−417.

(17) Dias, J. R. *Naturforsch.* **1989**, *44A*, 765−771.

(18) Borden, W. T.; Iwanmura, H.; Berson, J. A. *Acc. Chem. Res.* **1994**, *27*, 109.

(19) Roth, W. R.; Langer, R.; Ebbrecht, T.; Beitat, A.; Lennartz, H.-W. *Chem. Ber.* **1991**, *124*, 2751−2760.

(20) Dias, J. R. *Handbook of Polycyclic Hydrocarbons. Part A*; Elsevier: New York, 1987.

(21) Randic', M.; Trinajstic', N. *J. Am. Chem. Soc.* **1987**, *109*, 6923−6926. Randic', M. *Int. J. Quantum Chem.* **1980**, *17*, 549−586.

(22) Herndon, W. C. *J. Org. Chem.* **1981**, *46*, 2119−2125.

(23) Herndon, W. C. *Tetrahedron* **1973**, *29*, 3−12.

(24) Seitz, W. A.; Hite, G. E.; Schmalz, T. G.; Klein, D. J. *Graph Theory and Topology in Chemistry*; King, R. B., Rouvray, D. H., Eds.; Elsevier: Amsterdam, 1987; pp 458−465.

(25) Gao, Y.-D.; Herndon, W. C. *Mol. Phys.* **1992**, *77*, 585−599.

(26) Dowd, P.; Chang. W.; Paik, Y. H. *J. Am. Chem. Soc.* **1986**, *108*, 7416.

(27) Berson, J. A. *Angew. Chem., Int. Ed. Engl.* **1996**, *33*, 2750−2764.

(28) Dias, J. R. *J. Chem. Inf. Comput. Sci.* **1993**, *33*, 117−127.

(29) Dias, J. R. *J. Chem. Inf. Comput. Sci.* **1995**, *35*, 148−151.

(30) Ohkami, N.; Hosoya, H. *Theor. Chim. Acta* **1983**, *64*, 153−170.

(31) Dias, J. R. *J. Chem. Inf. Comput. Sci.* **1991**, *31*, 89−96.

(32) Klein, D. J. *Chem. Phys. Lett.* **1994**, *217*, 261−265.

(33) Hosoya, H.; Gao, Y.-D.; Nakada, K.; Ohuchi, M. *Fundamental Analysis of the Topological Dependency of the Electronic Structure of Conductive Polymer Networks. New Functionality Materials*, Tsuruta, T., Doyama, M., Seno, M., Eds.; Elseviers: Amsterdam, 1993; Vol. C, pp 27−34.

(34) Babic', D.; Gutman, I. *J. Math. Chem.* **1992**, *9*, 261−278.

(35) Dias, J. R. *Polycycl. Arom. Comput.* **1994**, *5*, 69−77.

(36) Balasubramanian, K. *J. Comput. Chem.* **1988**, *9*, 204−211.